PIER M

(Received 30 March 2024, Accepted 21 May 2024, Scheduled 5 June 2024)

Exploitation of the Spectral Stochastic Finite Element Model for the Evaluation of Surface Defects of the CFRP Composite

Zehor Oudni[1, 2, *] and Thinhinane Mahmoudi[1]

[1] *Department of Electrical Engineering, Mouloud Mammeri University of Tizi-Ouzou, Algeria*
[2] *Renewable Energy Management Laboratory (LMER), A. Mira University, Bejaia, Algeria*

ABSTRACT: This article deals with the detection of defects of rectangular geometric shape, in a carbon fiber reinforced polymer (CFRP) composite material based on non-destructive testing by eddy current (ECT). For this, a stochastic finite element calculation code is developed in a Matlab environment. The main objective is to evaluate the ECT signal of a fault by determining the impedance variation for the two configurations, in the absence and presence of a fault. Additionally, the impact of the direction of the carbon fibers is exploited to evaluate the reliability of the material. The validation of our work is carried out using experimental data from the work of Takagi et al., provided for reference.

1. INTRODUCTION

Composite materials are used in a variety of applications, e.g., in electronics, electricity, construction, aeronautics, automobiles, and sports. They are expected to replace traditional materials such as metals and ceramics that have dominated the industrial market so far. More and more they are being replaced by composite materials because of their advantages such as lightness, corrosion resistance, and design flexibility. Added to this is their good fatigue resistance and improved maintenance economy. A composite material consists of at least two distinct materials that are joined together, complementing each other and making it possible to obtain performances superior to those of a single material.

In general, a composite material consists of reinforcements (fibers, particles, fillers) embedded in a packaging called a matrix (polymeric matrix: thermoplastic, thermosetting or metal matrix: aluminium alloys, nickel-titanium alloys, or ceramic matrix: glass, cement) [1, 2].

The composite is found in various monolayer structures consisting of one or more identical plies assembled without any orientation, sandwiched with two thin skins but of high rigidity and low thickness containing a core of high thickness and low resistance or in laminates comprising multilayers whose fibers are oriented according to a given frame of reference [2–4].

However, these materials exhibit defects throughout their life cycle. Nondestructive testing (NDT) methods make it possible to control the quality of composites by detecting and characterizing defects, such as delamination, porosity and fibers breakage [4–6]. Many NDT methods exist such as ultrasonic (UT), radiographic (RT), and eddy current testing (ECT) which are widely used for material inspection [7–11].

Nondestructive testing (NDT) techniques are of great importance in assessing the quality and integrity of carbon fiber reinforced polymer (CFRP) materials.

Among the relevant techniques we cite:

1. Thermoelastic Stress Analysis (TSA):

TSA relies on the measurement of temperature changes induced by stress variations in the material. This process accurately detects the size and shape of defects.

2. Ultrasound Test (UT):

UT uses high frequency sound waves to inspect materials. This process provides precise information on the size and shape of defects.

3. Eddy Current Testing (ECT):

ECT uses electromagnetic induction to detect surface defects.

Although TSA and UT are accurate in detecting defects, ECT stands out as a viable solution due to its high inspection speed, efficiency, and reliability as well as the advantage of performing contactless testing [7–11].

The last technique cited, among other things "ECT", allows the appearance of an opposing current called eddy currents by the introduction of a current into a conductive material through a probe. This phenomenon is exploited in the technique of eddy current testing (ECT), by passing probes across the surface of materials for the detection of defects.

The present work is dedicated to the characterization of defects using ECT in a composite material, precisely in CFRP (carbon fiber reinforced polymer) [2].

CFRP is a type of composite material whose constituents are carbon fibers and polymer resin usually epoxy. The carbon fibers provide strength and rigidity, while the polymer resin acts as a binder by holding the fibers together. This results in a lightweight material with high strength, ideal for diverse

* Corresponding author: Zehor Oudni (z_mohellebi@yahoo.fr).

applications such as aerospace, automotive industry, and construction.

CFRP has several properties which are lightness, strength, rigidity, and corrosion resistance. It withstands high loads and stresses. It is one of the durable materials thanks to its resistance to corrosion, has an ability to withstand harsh environments, and facilitates molding into complex shapes.

The production of CFRP involves several stages. The first step is weaving the carbon fibers. Next step is impregnation in polymer resin, usually epoxy, to form a composite. This is then hardened at high temperatures and pressures to form a solid material.

Given the importance of CFRP in various industries, its characterization with a view to detecting defects that may occur is essential to ensure the reliability of the product made from this composite [2, 12].

In literature, different methods for modelling and simulating defects in composite materials by using ECT are described, e.g., analytical methods and numerical methods: finite difference method, boundary element method, volume integral, finite volume method, and finite element method.

In this article, we opted for a spectral stochastic finite element model (SSFEM), which allows the introduction of the electrical conductivity tensor. It was developed in a Matlab environment.

The exploitation of the SSFEM model is carried out through the identification of the electrical conductivity expressed by a conductivity tensor in the lengthwise, transverse, and orthogonal direction [2, 12].

The electrical conductivity in the transversal direction to the fibers is not zero (because there are contacts between the fibers), but it is less important than the conductivity in longitudinal direction of the fibres [2, 13].

SSFEM spectral stochastic finite element method is a random approach. The inputs of the modelling system are the random physical properties. In this study, the electrical conductivity tensor is considered Hermite polynomial. The response is given as random magnetic vector potential A [2, 12, 13].

The change in impedance is then derived by scanning the surface of the composite sample. A calculation of the probability of failure by using the reliability index is carried out in order to estimate the reliability of our material. The SSFEM model offers, on the one hand, an analysis of the problem posed in terms of responses resulting from resolution of the 2D axisymmetric equation and on the other hand an evaluation of the defect in terms of reliability directly after the analysis [10, 14]. This justifies our choice of SSFEM.

The results obtained during the simulations are compared to those provided by the experimental reference [15]. Thus, we obtain the validation of our stochastic model (SSFEM).

The reliability study begins with the calculation of the Beta (β), parameter characterizing the reliability of our study structure leading to the estimation of the probability of ruin [10]. The calculation process is illustrated in Figure 11 by a block diagram.

2. FORMULATION OF THE STOCHASTIC ALGEBRAIC SYSTEM

In this study, in an axisymmetric problem: we use a cylindrical reference (r, θ, z). If we have the following invariance θ, the quantities only depend on r and z.

The 2D magneto dynamic equation in (r, z) axis, considering harmonic hypothesis via magnetic vector potential $\vec{A}$, is performed as follows [2, 10, 14]:

$$-\frac{\partial}{\partial r}\left(\frac{\gamma}{r}.\frac{\partial\left(r.A_\phi\right)}{\partial r}\right)-\frac{\partial}{\partial z}\left(\frac{\gamma}{r}.\frac{\partial\left(r.A_\phi\right)}{\partial z}\right)+j\sigma\omega A_\phi=J_\phi \quad (1)$$

J_ϕ: The current density of the source [A.m^{-2}],
γ: Magnetic reluctivity [m·H^{-1}],
σ: Electric conductivity [S·m^{-1}].
$\omega = 2 * \pi * f$ [rad/s]; f: frequency [Hz].

Given that the magnetic vector potential $\vec{A}$ is the variable of the magneto dynamic equation in stochastic formulation to be solved, after solving the equation, the solutions obtained are in the Hermitian base, which results in the Hermetian formulation of $\vec{A}$. The calculation of the impedance Z is derived from the real and imaginary parts of the vector potential $\vec{A}$.

The magnetic vector potential $\vec{A}$ is expressed as a random variable in Hermit's polynomials. It is written as follows.

$$A=\sum_{\mathbf{i=0}}^{m_A}\mathbf{A_i\Psi_i}\left(\boldsymbol{\zeta_1},\cdots,\boldsymbol{\zeta_N}\right) \quad (2)$$

where $m_A = p - 1$ and p is the order of development of polynomial chaos.

The physical parameter σ_{stoch} considered as the hazard being the electrical conductivity, will be defined later and is developed on the basis of polynomial chaos. This distribution is carried out by exploiting the normal random variable represented by two coefficients, σ_{aveg} and S_d [2, 10]. It is expressed as Hermite polynomials as follows:

$$\sigma_{stoch}=\sum_{i=1}^{p-1}\sigma_{stoch_i}.H_i\left(\zeta_1,\ldots,\zeta_N\right) \quad (3)$$

The electrical conductivity is anisotropic in CFRP sheets because of the orientation of its fibers [12].

This results in a representation in matrix form. The elements of the matrix present electrical conductivity values that are quite large in the direction of the fibers and a hundred times less in the transverse direction [12], while the conductivity value is divided by a thousand their values in the direction orthogonal to the fiber plane compared to the values in the direction length [2]. In the following, the conductivity σ of a composite is represented by a tensor. The orientation of the carbon fibers is at an angle φ. The matrix which illustrates the generalized conductivity tensor of the composite is given below [12, 13, 16–19]:

$$[\sigma]=\begin{bmatrix}\sigma_{Lg}\cos^2\varphi+\sigma_{Tr}\sin^2\varphi & \frac{\sigma_{Lg}-\sigma_{Tr}}{2}\sin^2\varphi & 0\\ \frac{\sigma_{Lg}-\sigma_{Tr}}{2}\sin^2\varphi & \sigma_{Lg}\sin^2\varphi+\sigma_{Tr}\cos^2\varphi & 0\\ 0 & 0 & \sigma_{pli}\end{bmatrix} \quad (4)$$

As our study is devoted to the CFRP type composite, the orientation of the fibers is unidirectional in the direction of the x axis, which cancels the angle φ, [20, 21].

The conductivity tensor then becomes a diagonal matrix, and its representation is as follows: [2]:

$$[\sigma] = \begin{bmatrix} \sigma_{XX} & 0 & 0 \\ 0 & \sigma_{YY} & 0 \\ 0 & 0 & \sigma_{ZZ} \end{bmatrix} \quad (5)$$

where [12, 22, 23]

$$\sigma_{ZZ} \lll \sigma_{XX} \quad \text{and} \quad \sigma_{YY} \ll \sigma_{XX} \quad (6)$$

σ_{XX}: Represents the electrical conductivity in the lengthwise direction.

σ_{YY}: Represents the electrical conductivity in the width direction.

σ_{ZZ}: Represents the electrical conductivity in the thickness direction.

The considered CFRP with: $\{\sigma_{XX} = 50000; \sigma_{YY} = 100; \sigma_{ZZ} = 50\}$ [S·m^{-1}] is represented by the following tensor [2, 12, 15, 16]:

$$[\sigma_{\text{CFRP}}] = \begin{bmatrix} 50000 & 0 & 0 \\ 0 & 100 & 0 \\ 0 & 0 & 50 \end{bmatrix} \quad (7)$$

In this application, three hypotheses are taken into account [2]:

- Electrical conductivity is considered as an average a value 'σ_{aveg}'.
- The longitudinal electrical conductivity dominates in the tensor.
- The standard deviation S_d is a ratio of the average electrical conductivity.

Considering these hypotheses, the electrical conductivity tensor which represents the stochastic matrix becomes [10]:

$$\sigma_{stoch} = \begin{bmatrix} \sigma_{aveg} & S_d & 0 \\ S_d & \sigma_{aveg} & 2 * S_d \\ 0 & 2 * S_d & 2 * \sigma_{aveg} \end{bmatrix} \quad (8)$$

After development and integration of the conductivity tensor in stochastic matrix form, we obtain the following configuration of a matrix system [10, 14]:

$$\begin{bmatrix} D_{00}^{st} & D_{01}^{st} & D_{12}^{st} \\ D_{01}^{st} & D_{11}^{st} & D_{21}^{st} \\ D_{02}^{st} & D_{12}^{st} & D_{22}^{st} \end{bmatrix} \begin{bmatrix} A_{P0} \\ A_{P1} \\ A_{P2} \end{bmatrix} = \begin{bmatrix} S_0 \\ S_1 \\ S_2 \end{bmatrix} \quad (9)$$

where A_{P0}, A_{P1}, A_{P2} are the solutions of the stochastic complex algebraic system, and S_0, S_1, S_2 are the source vector components [10, 14]:

$$\begin{aligned} P_{jk}^{s} &= K_{jk}^{s} + j\omega L_{jk}^{s} \\ k &= 0, \ldots, p-1; \quad j = 0, \ldots, p-1 \end{aligned} \quad (10)$$

K_{jk}^{s}, L_{jk}^{s} are the random linear matrixes related to solving problem.

3. ANALYSIS OF RESPONSES

After solving the matrix system, three random solutions of the potential vector A_P are obtained: A_{P0}, A_{P1}, A_{P2}.

The number of solutions is equal to p, which represents the degree of chaos polynomial.

In the first step, the impedance Z_{CFRP} is calculated in the plate without defects and then in the zone supposed to present a defect, according to the following expression:

$$Z_{\text{CFRP}} = \text{Real}\,(Z_{\text{CFRP}}) + \text{Imag}\,(Z_{\text{CFRP}}) \quad (11)$$

$$\text{Real}\,(Z_{\text{CFRP}}) = \frac{N_c^2}{J_{ex} \cdot {S_c}^2} \omega \iint_{s_c} 2 \cdot \pi \cdot r \cdot \text{Imag}\,(A_P) \cdot dS_c \quad (12)$$

$$\text{Imag}\,(Z_{\text{CFRP}}) = \frac{N_c^2}{J_{ex} \cdot {S_c}^2} \omega \iint_{S_c} 2 \cdot \pi \cdot r \cdot \text{Real}\,(A_P) \cdot dS_c \quad (13)$$

J_{ex}: Current density [A/m^2], S_c: Conductors Section [m^2], N_c: Number of turns, r: Inductor radius [mm].

To evaluate the safety state of the system studied, we calculate the function G_{SSFEM} from the solutions obtained by the stochastic development, and its expression is given as follows: [2, 14],

$$G_{SSFEM} = (Z_{PL}) - \sum_{j=0}^{p-1} Z_j^{is} \Psi_j\,(\zeta_1, \zeta_2) \quad (14)$$

$$Z_{Def} = \sum_{j=0}^{p-1} Z_j^{is} \Psi_j\,(\zeta_1, \zeta_2) \quad (15)$$

Z_{pL}: impedance without defaults, Z_{Def}: impedance stochastic in presence of defect.

The reliability index β is calculated from the limit state function G_{ISFEM} [24, 25].

$$\beta = \text{Min}\left(\lceil G_{\text{SSFEM}} \rceil^{\frac{1}{2}}\right) \quad (16)$$

From literature, the reliability index is known to be the reliability degree parameter of a system [24].

For values of reliability index greater than 3, the system is in a state of reliability, and on the other hand when these values are lower than 3, the reliability is not verified any more. The failure probability is higher than zero, and both curves indicate clearly when the reliability of the system is good [24–26].

4. DESCRIPTION OF THE APPLICATION

The application consists of characterizing a CFRP composite type specimen, in the presence and absence of defects.

The scan is carried out by moving a differential sensor made up of two coils above the area presenting a defect. The parameters taken into account during the simulations are identical to those presented by the reference experiment [15].

Table 1 brings together all the elements used during the tests.

The results obtained in terms of impedance variation are compared with those presented by experiment and are presented in Table 2.

Figure 1 presents the geometric device studied under the 2D axisymmetric hypothesis [14].

TABLE 1. Configurations of coil and plate [2].

Coil	Inner diameter	Outer diameter	Height	Width	Current	Number of turns
	1.2 mm	3.2 mm	0.8 mm	1.0 mm	1/140 A	140
Plat	Height	Widt	Thickness	Relative permeability		
	40 m	40 mm	1.25 mm	1		
Defect			Length	Width	Depth	
			10 mm	0.2 mm	1.25 mm	
Lift-off		0.5 mm	Frequency		300 kHz	

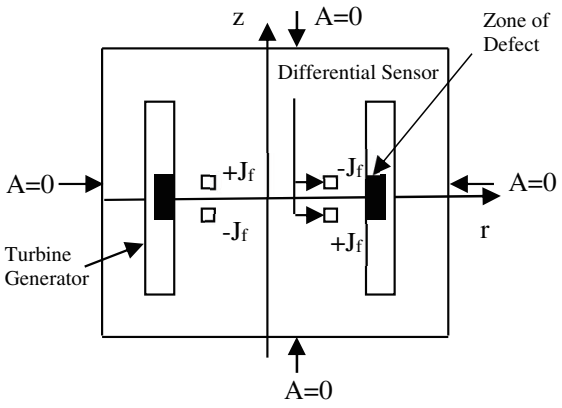

FIGURE 1. Geometry of the study device in $(r,\ z)$ plane.

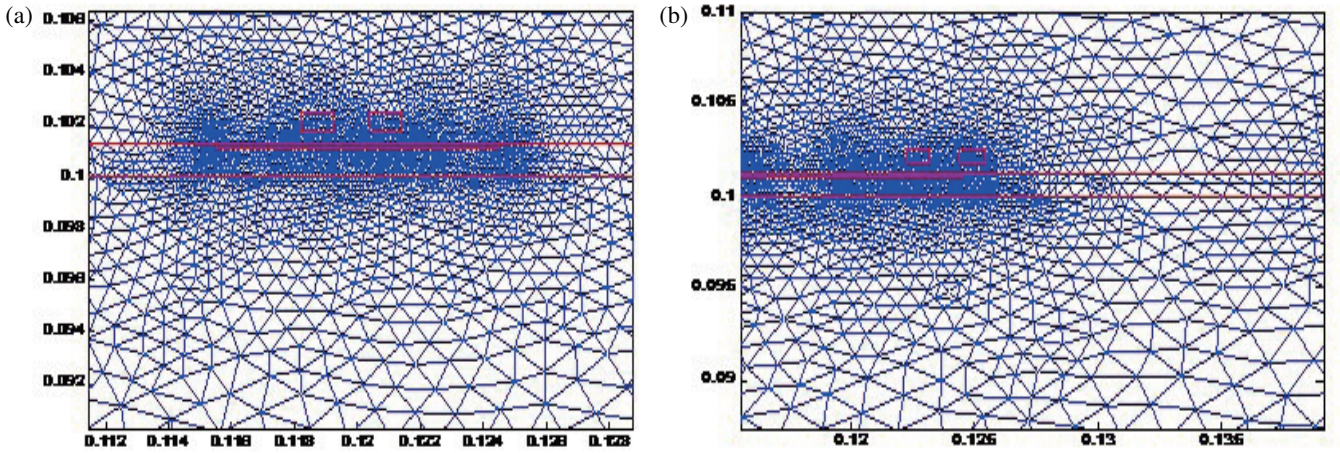

FIGURE 2. Geometry mesh. (a) at the 5th iteration, (b) at the 9th iteration.

5. RESULTS AND INTERPRETATION

The mesh of the NDT-EC structure, with displacement of the differential sensor with a step of 0.01 is represented in Figure 2.

The mesh is produced at each iteration automatically with a refined mesh in the defect region.

The characteristics of the resolution domain mesh are the number of nodes which is **4959**, and the number of triangles is **9840**.

After solving, three solutions in terms of magnetic vector potential are obtained: A_0, A_1, and A_2. The values of the resistance variation: ΔR_0, ΔR_1, and ΔR_2 and of the reactance variation ΔX_0, ΔX_1, and ΔX_2 are calculated from the solution.

This generates the different variations of the impedance DELTAZ0, DELTAZ1, DELTAZ2 of dimension n_p corresponding to the order of the considered Hermite polynomial.

Figure 3 shows the three solutions of the magnetic vector potential.

Both impedance resulting from the SSFEM models and those obtained by the experimental data of the Benchmark JSAEM#Problème1 [15] are presented in Figure 4.

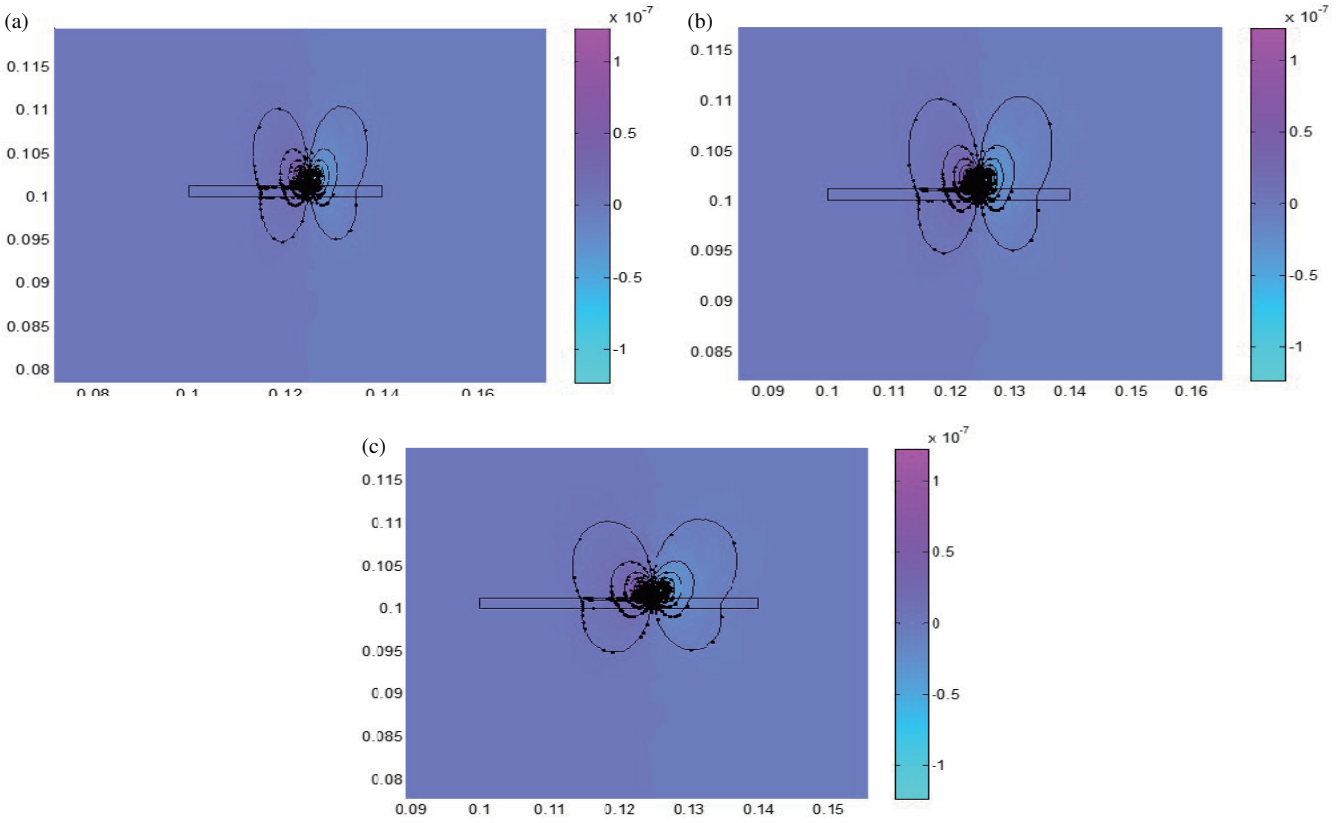

FIGURE 3. Stochastic solutions of vector potential A, (a) $p = 0$, (b) $p = 1$, (c) $p = 2$.

TABLE 2. The predictions of the coil impedance variation.

Impedance Experiment [12]	$Z_{\text{Exp}} = -2.22 + 2.7i\ [\Omega]$
Impedance Simulation SSFEM	$Z_{\text{SSFEM}} = -2.15 + 2.32i\ [\Omega]$
Frequency	300 kHz
Lif-Off	0.5 mm

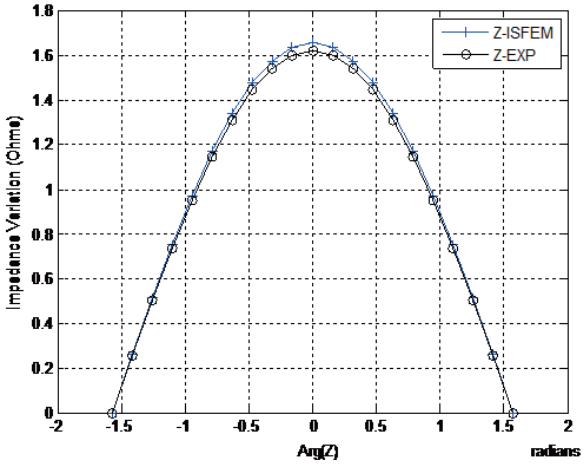

FIGURE 4. Comparison between stochastic and experimental impedance.

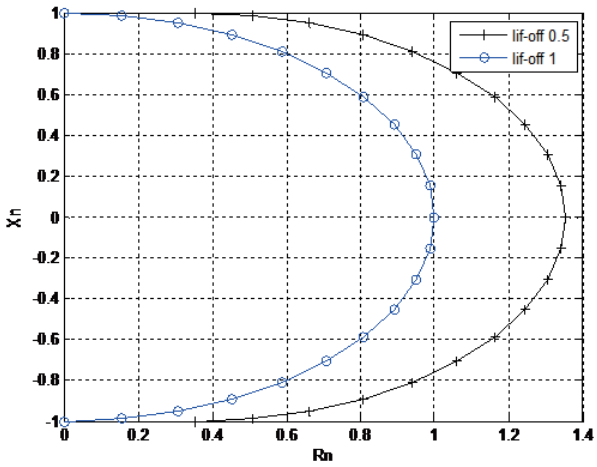

FIGURE 5. Representation of the real part normalized according to the imaginary part of the impedance Z for two lift-Off values.

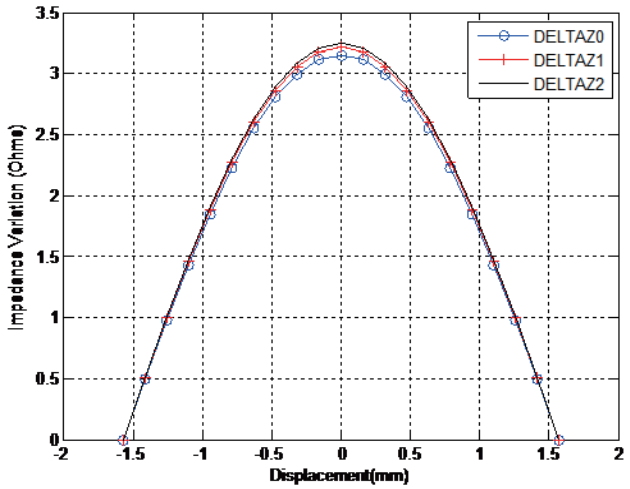

FIGURE 6. Different variations of stochastic impedances in the fault zone.

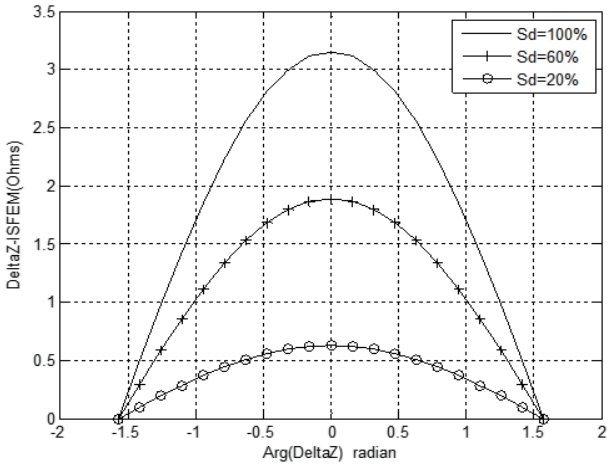

FIGURE 7. Representation of DELTAZ0 for different standard deviations in the fault zone.

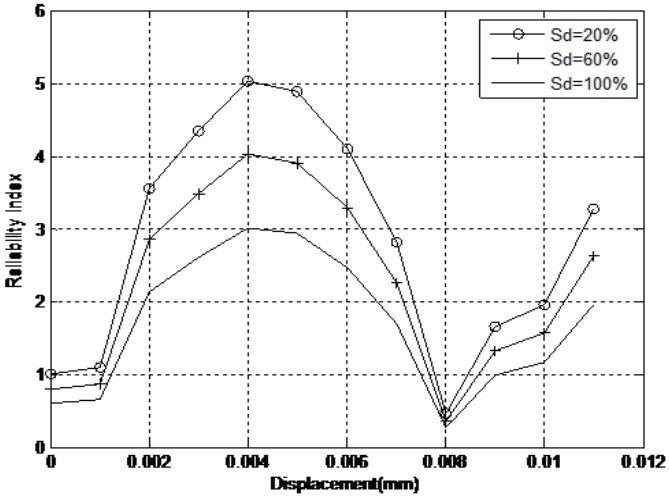

FIGURE 8. Profile of reliability index according to the sensor displacement in the fault zone for different standard deviations.

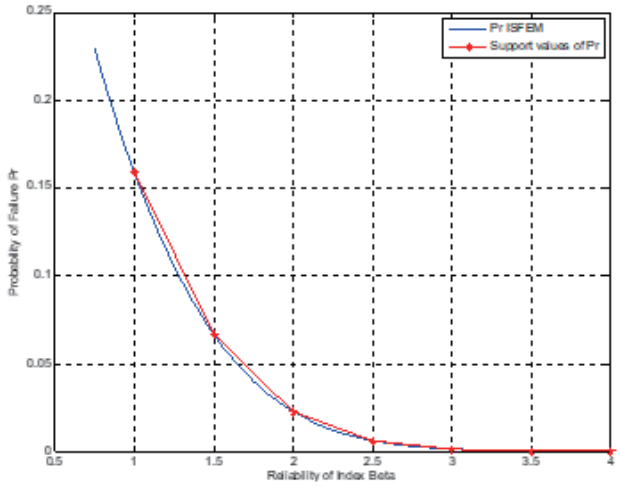

FIGURE 9. Trend of the probability of failure according to the reliability index.

The results are in good agreement. The accuracy and precision prove the robustness of stochastic model SSFEM.

Figure 5 denotes the impedance profile in Nyquist diagram, imaginary part of impedance via real part of impedance for different values of lift-off 0.5 mm and 1 mm.

The three solutions of stochastic impedances are presented in Figure 6, by DELTAZ0, DELTAZ1, and DELTAZ2. It is noticed that there is difference between 0-order solution and the second order one.

For the next step, the solution DELTAZ0 is used for the analysis of reliability system. Figure 7 denotes the impedance variation, DELTAZ0 for different standard deviations $Sd = 100\%$, $Sd = 60\%$, $Sd = 20\%$.

It is noticed that for high standard deviation values, the impedance variation is greater. This informs on the importance of the defect in the suspicious zone.

Reliability is approached by calculating the reliability index for different standard deviations. It is remarked that the risk of failure is greater for a 100% defect, in case of total lack of material.

The influence of the standard deviation of the reliability index is illustrated in Figure 8. Three standard deviation values are considered 0.2, 0.6, and 1.

Figure 8 shows the high risk of the defect presence [2]. In this case, the standard deviation is high, and the reliability index is low.

Figure 9 shows the probability failure Pr behavior of the inspection situation. The results are obtained using a program developed under Matlab environment. The reliability index main objective is to correlate the reliability index through Lagrange polynomial using reference data [25,26].

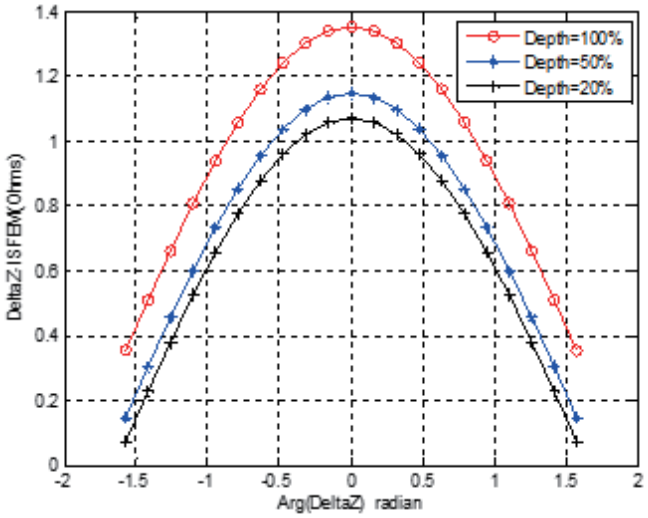

FIGURE 10. Influence of the depth of the defect on the variation of the impedance.

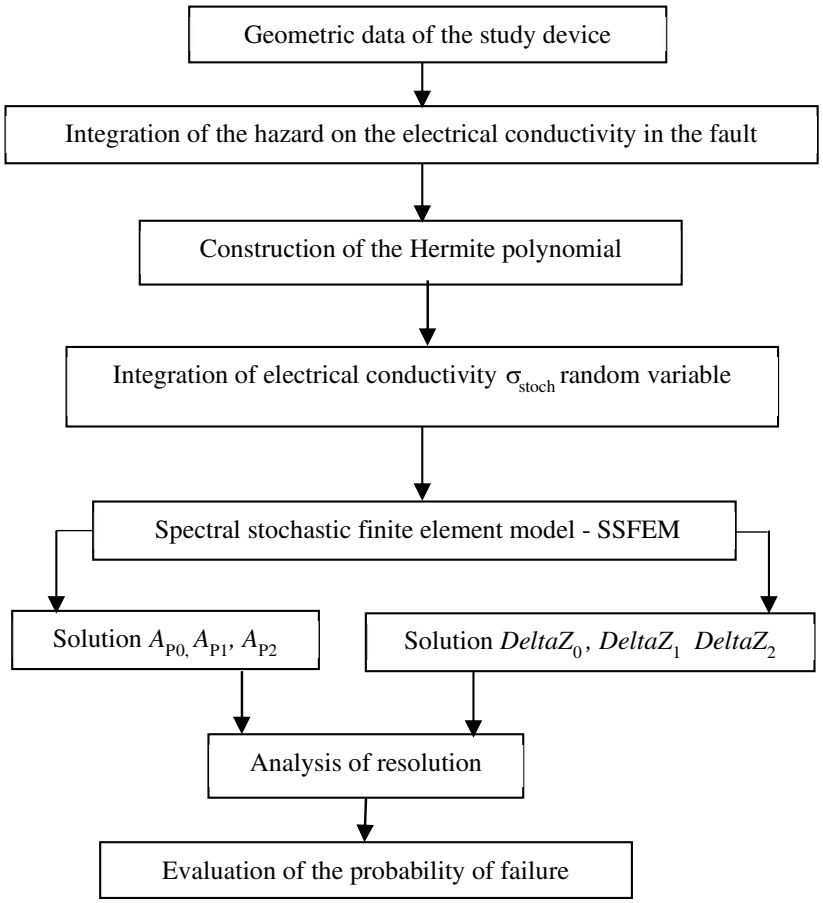

FIGURE 11. SSFEM calculation process diagram.

The Pr values are obtained using reliability index, calculated via stochastic computation (SSFEM).

The calculation of the probability of failure is carried out using the Lagrange polynomial. Other methods can be used such as the FORM method [25, 26].

The Lagrange polynomial is constructed from reference data in terms of the index β and the probability Pr, cited in [26], associated with those obtained by the SSFEM model.

The construction of the Lagrange polynomial leads to a direct correlation between the reliability index and the probability of failure.

The evolution of the failure probability is plotted according to the reliability index and provided in Figure 9. The comparison is then performed with a curve obtained from reference data [26] (Figure 9). The results are in good agreement.

From value of $\beta \geq 3$, Pr becomes lower, which leads to ensuring the reliability.

Figure 10 illustrates the influence of the depth of the defect on the variation of the impedance. Considering that the initial defect depth, given in table 1, is 100% (1,25 mm), we carried out simulations for two depths of 50% and 40% of the initial value.

We see that the impedance variation increases with the defect depth rate.

Figure 11 describes the different steps of the spectral stochastic finite element (SSFEM) calculation code.

6. CONCLUSION

The present study proposes a numerical model based on finite elements in uncertain environments. This model, called spectral stochastic finite element method (SSFEM), is developed by modifying the source codes available in the finite element method.

The main objective of this development is to ensure the characterization of defects likely to be present on a CFRP type composite material.

To carry out this fault detection, nondestructive testing by eddy current (NDT-EC) is used. The differential sensor made it possible to provide us with indications concerning the variation of the impedance in the plate without a fault and with the presence of a fault.

Modeling in an uncertain environment provides for the random nature of the physical property of the material which is electrical conductivity, itself developed in the basis of the Hermite polynomial in polynomial chaos. This distribution is produced by the Gaussian variable characterized by a mean value and a standard deviation. The results obtained for a standard deviation of 100% by the different simulations are compared with those provided by the reference JSAEM#Problem1 [15], and the observation is more than satisfactory. This helps to reinforce the SSFEM model. Following these satisfactory results, other simulations were carried out for standard deviations 20% and 60% in order to demonstrate the impact of the value of the standard deviation on the importance of the defect.

After the analysis of the system in terms of presence of fault by the SSFEM model, a reliability calculation was started directly by exploiting the variation of the impedance and by calculating the probability of failure by demonstrating its correlation with the beta reliability index. The results of the reliability evaluation are in agreement with the expected theoretical results. This strengthens our spectral stochastic model by validating the codes developed in Matlab.

It is important to note that our proposal of the SSFEM model has the advantage of characterizing defects at different thicknesses supported by NDT-EC, compared to other already existing stochastic methods that rely on the inverse problem.

We can affirm that the simulations carried out by the spectral stochastic model consume relatively five (05) times less time than the Monte Carlo simulation method or the Latin hypercube.

REFERENCES

[1] Rajak, D. K., D. D. Pagar, R. Kumar, and C. I. Pruncu, "Recent progress of reinforcement materials: A comprehensive overview of composite materials," *Journal of Materials Research and Technology*, Vol. 8, No. 6, 6354–6374, 2019.

[2] Mahmoudi, T., Z. Oudni, A. Berkache, and J. Lee, "Characterization of defects in composite materials by the intrusive stochastic method using the gaussian type random variable," *Przeglad Elektrotechniczny*, Vol. 99, No. 3, 246, 2023.

[3] Galehdar, A., W. Rowe, K. Ghorbani, P. J. Callus, S. John, and C. H. Wang, "The effect of ply orientation on the performance of antennas in OR on carbon fiber composites," *Progress In Electromagnetics Research*, Vol. 116, 123–136, 2011.

[4] Holloway, C. L., M. S. Sarto, and M. Johansson, "Analyzing carbon-fiber composite materials with equivalent-layer models," *IEEE Transactions on Electromagnetic Compatibility*, Vol. 47, No. 4, 833–844, 2005.

[5] Wen, J., Y. Zeng, C. Wu, J. Guan, and H. Guo, "Silk lattice structures from unidirectional silk fiber-reinforced composites for breaking energy absorption," *Advanced Engineering Materials*, Vol. 22, No. 3, 1900921, 2020.

[6] Galos, J., "Thin-ply composite laminates: A review," *Composite Structures*, Vol. 236, No. 3, 111920, 2020.

[7] Bui, H. K., G. Wasselynck, D. Trichet, and G. Berthiau, "Application of degenerated hexahedral Whitney elements in the modeling of NDT induction thermography of laminated CFRP composite," *IEEE Transactions on Magnetics*, Vol. 52, No. 3, 1–4, 2016.

[8] Bowkett, M. and K. Thanapalan, "Comparative analysis of failure detection methods of composites materials' systems," *Systems Science & Control Engineering*, Vol. 5, No. 1, 168–177, 2017.

[9] Berkache, A., J. Lee, D. Wang, and D.-G. Park, "Development of an eddy current test configuration for welded carbon steel pipes under the change in physical properties," *Applied Sciences*, Vol. 12, No. 1, 93, 2022.

[10] Oudni, Z., A. Berkache, H. Mehaddene, H. Mohellebi, and J. Lee, "Comparative study to assess reliability in the presence of two geometric defect shapes for non-destructive testing," *Przegląd Elektrotechniczny*, Vol. 95, No. 12, 48–52, 2019.

[11] García-Martín, J., J. Gómez-Gil, and E. Vázquez-Sánchez, "Non-destructive techniques based on eddy current testing," *Sensors*, Vol. 11, No. 3, 2525–2565, 2011.

[12] Versaci, M., G. Angiulli, P. Crucitti, D. D. Carlo, F. Laganà, D. Pellicanò, and A. Palumbo, "A fuzzy similarity-based approach to classify numerically simulated and experimentally detected carbon fiber-reinforced polymer plate defects," *Sensors*, Vol. 22, No. 11, 4232, 2022.

[13] Hachi, D., N. Benhadda, B. Helifa, I. K. Lefkaier, and B. Abdelhadi, "Composite material characterization using eddy current by 3D FEM associated with iterative technique," *Advanced Electromagnetics*, Vol. 8, No. 1, 8–15, 2019.

[14] Oudni, Z., M. Féliachi, and H. Mohellebi, "Assessment of the probability of failure for EC nondestructive testing based on in-

trusive spectral stochastic finite element method," *The European Physical Journal — Applied Physics*, Vol. 66, No. 3, 30904, 2014.

[15] Takagi, T., M. Hashimoto, H. Fukutomi, M. Kurokawa, K. Miya, H. Tsuboi, M. Tanaka, J. Tani, T. Serizawa, Y. Harada, E. Okano, and R. Murakami, "Benchmark models of eddy current testing for steam generator tube: Experiment and numerical analysis," *International Journal of Applied Electromagnetics in Materials*, Vol. 5, No. 3, 149–162, 1994.

[16] Park, J. B., T. K. Hwang, H. G. Kim, and Y. D. Doh, "Experimental and numerical study of the electrical anisotropy in unidirectional carbon-fiber-reinforced polymer composites," *Smart Materials and Structures*, Vol. 16, No. 1, 57, Nov. 2006.

[17] Chebbi, H. and D. Prémel, "The fast computation of eddy current distribution and probe response in homogenized composite material based on semi-analytical approach," *The European Physical Journal Applied Physics*, Vol. 89, No. 1, 10901, 2020.

[18] Burningham, C. A., C. P. Pantelides, and L. D. Reaveley, "Repair of reinforced concrete deep beams using post-tensioned CFRP rods," *Composite Structures*, Vol. 125, 256–265, 2015.

[19] Dufour, I. and D. Placko, "Separation of conductivity and distance measurements for EC-NI of graphite composite materials," *J. Phys. III France*, Vol. 3, No. 6, 1065–1074, 1993.

[20] Liberati, A. C., P. Patel, A. Roy, P. Vo, C. Pan, C. Moreau, R. R. Chromik, S. Yue, and P. Stoyanov, "Effect of carbon fiber orientation when cold spraying metallic powders onto carbon fiber-reinforced polymers," *Journal of Thermal Spray Technology*, Vol. 33, 596–608, 2024.

[21] Newton, M., T. Chowdhury, I. Gravagne, and D. Jack, "Nondestructive evaluation of in-plane waviness in carbon fiber laminates using eddy current testing," *Applied Sciences*, Vol. 13, No. 10, 6009, 2023.

[22] Karpenko, O., A. Efremov, C. Ye, and L. Udpa, "Multi-frequency fusion algorithm for detection of defects under fasteners with EC-GMR probe data," *NDT & E International*, Vol. 110, 102227, 2020.

[23] Ajith, G. and D. Ghosh, "A novel method for solving nonlinear stochastic mechanics problems using FETI-DP," *International Journal for Numerical Methods in Engineering*, Vol. 123, No. 10, 2290–2308, 2022.

[24] Loève, M., *Graduate Texts in Mathematics] Probability Theory I*, Vol. 45, No. Chapter 8, 353–405, 1977.

[25] Silva Jr., C. R. A., "Application of the galerkin method to stochastic bending of kirchhoff plates," Ph.D. dissertation, 2004.

[26] Da Silva Jr., C. R. A., A. T. Beck, and E. D. Rosa, "Solution of the stochastic beam bending problem by Galerkin method and the Askey-Wiener scheme," *Latin American Journal of Solids and Structures*, Vol. 6, No. 1, 51–72, 2009.